

CO₂ emissions and uptake in rendering mortars: sustainable approach

Emissões e captura de CO₂ em argamassas de revestimento: abordagem sustentável

Beatrice Lorenz Fontolan 

Taine Beal Silva 

Giovanna Patrícia Gava 

Eduardo Rigo 

Alex Neves Junior 

Edna Possan 

Abstract

This study aimed to estimate CO₂ emission and uptake due to the mixed rendering mortars carbonation process, replacing natural aggregate (NA) with recycled aggregate (RA) and lime contents to produce less emissive final material. Mortars were subjected to natural carbonation in three environments. Carbonation depth was evaluated until 119 days of CO₂ environmental exposure, and thermogravimetric analysis determined absorbed carbon content. The scenario evaluation considered different depths for the potential CO₂ uptake. It was found that the higher the lime content, the higher the carbon emissions and capture. However, the CO₂ captured amount (25.41 KgCO₂/m³) does not balance its emission from raw materials production. Replacing NA for RA, the mortars reduced emissions associated with production by approximately 8.15%. The scenario simulation proved that constructive control is essential for rendering mortar depths less than 20 mm, the maximum carbon fixation is reached before rendering. Mortars with recycled aggregate are less emissive, which is essential in selecting more sustainable building materials.

Keywords: CO₂ sequestration. Sustainability. Compensatory measures. Construction waste.

Resumo

Este estudo teve como objetivo estimar a emissão e captura de CO₂ devido ao processo de carbonatação de argamassas mistas, substituindo agregado natural (AN) por agregado reciclado (AR) e teores de cal para produzir material final menos emissivo. As argamassas foram submetidas à carbonatação natural em três ambientes. A profundidade de carbonatação foi avaliada aos até 119 dias de exposição ao tempo com presença de CO₂, e a análise termogravimétrica determinou o teor de carbono absorvido. A avaliação dos cenários considerou diferentes profundidades para o potencial absorção de CO₂. Verificou-se que quanto maior o teor de cal, maiores as emissões e captura de carbono. Contudo, a quantidade de CO₂ capturada (25,41 KgCO₂/m³) não neutraliza a sua emissão proveniente da produção de matérias-primas. Substituindo o AN pelo AR, as argamassas reduziram as emissões associadas à produção, em aproximadamente 8,15%. A simulação dos cenários comprovou que o controle construtivo é essencial, pois em espessuras inferiores a 20 mm a fixação máxima de carbono é alcançada antes da aplicação de revestimento. As argamassas com agregados reciclados são menos emissivas, o que é essencial na seleção de materiais de construção mais sustentáveis.

Palavras-chave: Sequestro de CO₂. Sustentabilidade. Medidas compensatórias. Resíduos de construção.

¹Beatrice Lorenz Fontolan

¹Universidade Tecnológica Federal do Paraná
Curitiba - PR - Brasil

²Taine Beal Silva

²Universidade Tecnológica Federal do Paraná
Pato Branco - PR - Brasil

³Giovanna Patrícia Gava

³Universidade Estadual do Oeste do Paraná
Cascavel - PR - Brasil

⁴Eduardo Rigo

⁴Universidade Federal da Integração Latino-Americana
Foz do Iguaçu - PR - Brasil

⁵Alex Neves Junior

⁵Universidade Federal de Mato Grosso
Cuiabá - MT - Brasil

⁶Edna Possan

⁶Universidade Federal da Integração Latino-Americana
Foz do Iguaçu - PR - Brasil

Recebido em 25/03/23

Aceito em 13/08/23

Introduction

The construction industry (CI) is one of the most significant contributors to anthropogenic emissions. Only the cement industry is globally responsible for about 7% of all carbon dioxide emissions (IEA; WBCSD, 2018). CO₂, a major Greenhouse Gas (GHG), is responsible for increasing the average planet temperature and consequent global warming (IPCC, 2021). Several carbon capture processes have been studied to reduce the impacts associated with CO₂ emissions. One of them is the carbonation reaction method (recarbonation), which in cement-based materials corresponds to CO₂ reaction from the atmosphere with alkaline compounds such as calcium hydroxide and portlandite (Ca(OH)₂) present in the cementitious material, forming calcium carbonate (CaCO₃) and water (H₂O (Wijayasundara; Mendis; Ngo, 2017; Yang; Seo; Tae, 2014)). This reaction also occurs in lime-based materials, where calcium and magnesium hydroxides may be present, depending on the rock mineralogical origin used in lime production (Ergenç; Fort, 2018; Kang; Kwon; Moon, 2019).

In Brazil, it is common the use lime in mortars, due to its satisfactory properties, such as lower drying shrinkage and greater water retention, workability, and plasticity (Chever; Pavia; Howard, 2010). Cement and hydrated lime rendering mortars are very porous, allowing the rapid diffusion of atmospheric CO₂ into the matrix when applied in small thicknesses, which favors CO₂ fixation by the natural carbonation process. However, in a high porosity network, CO₂ capture is also intertwined with the chemical composition (Ergenç; Fort, 2018 Kang; Kwon; Moon, 2019; Borges *et al.*, 2023). CO₂ may chemically react with (Ca(OH)₂) and Mg(OH)₂, forming calcium carbonate (CaCO₃) and magnesium carbonate (MgCO₃), respectively (Delabona; Gava; Rufatto, 2020; Fontolan; Gava; Silva, 2020).

Environmental aspects demand solutions for low-carbon materials (Coppola *et al.*, 2019). According to Fukui *et al.* (2013), the amount of CO₂ released from mortar production is directly proportional to the cement and hydrated lime percentage in its composition. The use of these materials ought to be balanced (Forster *et al.*, 2020; Maddalena; Roberts; Hamilton, 2018). Cement emission in Brazil is around 564 kg per ton of product (IEA; WBCSD, 2018), and lime emission range from 607 to 2169 kg per ton of product due to the different technologies and combustion materials used and the raw materials' decarbonation. The high lime emission is due to the lack of efficiency and control of the lime kiln used in manufacturing, which varies according to the type and amount of energy consumed (John; Punhagui; Cincotto, 2014).

Approximately 50% of the cement produced in Brazil is used for mortar production, whereas 4% is industrialized and 96% is made on-site (Punhagui *et al.*, 2018) by artisanal and not controlled techniques. According to Sindicato Nacional da Indústria do Cimento (SNIC, 2022), the Brazilian construction sector produced 65.80 million tons of cement in 2020. That is 28.08 million tons of cement destined for mortar production. Based on a standard mortar mix (1:1:6), the demand is 167 million tons of sand. Considering that 50% of mortars at the end of their life cycle turn into fine aggregate, 83.56 million tons of RA are generated with potential use in mortar - a non-structural material used in Brazil in large volume - production.

Literature studies (Šavija; Luković, 2016; Shin; Kim, 2022) indicate the technical and economic feasibility of using recycled fine aggregates (RA) in rendering and/or laying mortar production. Their use in mortar production minimizes associated waste's environmental impacts Costa and Ribeiro (2020). It contributes to the CO₂ capture process due to the existence of chemical compounds that can undergo carbonation. Construction and demolition waste has calcium hydroxide (Ca(OH)₂) and hydrated calcium silicate (C-S-H) in its composition, contributing to carbonation chemical reaction development (Cai; Wang; Xiao, 2018). Using RA in cementitious materials reduces CO₂ emissions by increasing waste utilization. When demolished RAs are not fully carbonated, they may increase the potential for CO₂ capture when used as aggregates. In this process, new surfaces are exposed, and a new carbonation cycle begins, fixing CO₂ from the atmosphere (Kaliyavaradhan; Ling, 2017).

The CO₂ captured by recarbonation can be quantified indirectly based on the carbonated depth or directly by TGA (Possan, 2019). Thermogravimetric analysis (TGA) is a powerful method for determining the amount of carbonate material amount present in concrete and mortars. Calcium carbonate decomposition analysis allows for studying the cementitious materials samples' carbonation and CO₂ absorption (Villain; Thiery; Platret, 2007). Such a method is feasible for determining the cement-based materials' carbonation degree; it quantifies the calcium carbonate content in a sample extracted from concrete mortar and reduced to powder. By the derived curve (DTG), the potential CO₂ capture is obtained by balancing the mass lost between the carbonated and non-carbonated samples (Mazurana *et al.*, 2021; Neves Junior *et al.*, 2019).

Some studies (Mazurana *et al.*, 2021; Borges *et al.*, 2023) have evaluated CO₂ capture in rendering mortars with different RA contents. Mazurana *et al.* (2021) evaluated CO₂ capture in mortars with RA and hydrated

lime using thermogravimetry and reported that rendering mortar samples exposed to the action of atmospheric CO₂ resulted in carbonate depths ranging from 3 mm to 20 mm at 28 days of natural carbonation, depending on the mortars' ratio. Borges *et al.* (2023) evaluated carbon capture by carbonation in cementitious mortars with three granulometric distributions of recycled aggregates and found that CO₂ capture was higher in matrices with 100% recycled aggregate.

The studies did not approach the influence of hydrated lime content on CO₂ capture and did not evaluate projections to later ages based on the thermogravimetric method. Hydrated lime is widely used in Brazil and several countries where masonry construction system is coated with mortar. Lime production contributes to significant CO₂ due to the decarbonization and the use of fossil fuels and/or wood burning. Understanding how this material influences CO₂ emissions and capture due to mineralization in the life cycle is relevant for the selection of the material that leads to less emissive mortar production. This study can also help to fit materials to ease carbon capture throughout the building life cycle.

Andrade *et al.* (2018) studied rendering mortars with RA without hydrated lime using analytical equations based on the samples' carbonation depth and reported that rendering mortar samples exposed to the action of atmospheric CO₂ resulted in carbonate depths ranging from 3 mm to 20 mm at 250 days of natural carbonation.

Further studies are needed to determine potential CO₂ uptake in cement and lime-based rendering and laying mortars to assess its influence and the exposure environment. By thermogravimetric analysis, this research aims to estimate the amount of CO₂ captured, in rendering mortars produced with different lime contents and with natural aggregate replaced by different fine aggregate contents from construction demolition waste, exposed to natural carbonation. By evaluating the CO₂ emissions and potential capture of rendering mortars with construction and demolition waste over time, this study converges with the Paris Agreement's goal, signed at the 21st United Nations Framework Convention on Climate Change (UNFCCC). The agreement intends to limit global warming to 1.5 °C above pre-industrial levels by reducing GHGs, especially anthropogenic carbon dioxide emissions. The Sustainable Development Goals (SDGs) 12 – Responsible Consumption and Production and 13 – Action United Nations are also within the research's scope. Studying the CO₂ capture in cement-based mortars and the influence of lime and recycled aggregate on it, it's important in the current context. In addition, promoting the utilization of waste materials in the construction industry can help offset a portion of the emissions generated during the manufacturing of construction materials.

Material and methods

Materials and mortars' production and characterization

To evaluate the CO₂ uptake in rendering mortars, 40 x 40 x 160 mm prismatic specimens were produced as per Table 1. Each specimen is classified based on its lime content and whether it consists solely of natural sand (NA) or includes recycled aggregate (RA). Pozzolanic Portland cement (CP II – Z – 32, similar to ASTM C-595 I P), dolomitic lime (CH-III), quartz-origin natural sand, and RA (Figure 1) were used as per the chemical and physical characteristics shown in Table 2.

Table 1 - Materials consumption for 1m³ of rendering mortar production

Mortar	Lime proportion	RA (%) *	Consumption (kg/m ³)				
			Cement	Lime	NA	RA	Water
0.5L-NA	0.5	0	174.8	61.4	1543.6	-	335.6
1.0L-NA	1	0	168	117.6	1483.3	-	324.31
2.0L-NA	2	0	156.7	219.4	1383.6	-	341.3
1.0L-RA	1	25	162.9	114.1	1078.6	328.6	319.3

Note: NA: Natural Aggregate | RA: Recycle Aggregate | * In relation to natural aggregate mass.

Figure 1 - Materials used in mortar production



Table 2 - Materials' Physico-chemical composition

	Material	Cement	Lime	RA	NA
Chemical composition (%)	CaO	53.7	45.1	10.3	-
	SiO ₂	19.7	1.1	64.7	-
	Al ₂ O ₃	6.5	-	9.1	-
	SO ₃	3.6	-	0.5	-
	Fe ₂ O ₃	3.3	0.2	5.1	-
	MgO	3.2	22.0	0.1	-
	K ₂ O	1.1	0	0.6	-
	TiO ₂	0.4	<0.1	1.2	-
	SrO	0.1	<0.1	<0.1	-
	MnO	0.1	<0.1	0.1	-
	BaO	0.1	-	-	-
	ZnO	<0.1	-	<0.1	-
	CuO	-	-	<0.1	-
L.O.I.*	8.05	31.54	8.3	-	
Characteristi	Dusty material content (%)	-	-	5.93	0.3
	Maximum diameter (mm)	-	-	4.75	1.18
	Fines (%)	-	-	2.31	1.6
	H ₂ O absorption (%)	-	-	10.48	1.2
	Bulk density (g/cm ³)	1.04	0.73	1.28	1.53
	Dry density (g/cm ³)	2.96	2.44	2.32	2.67

Note: *Loss on ignition | RA: Recycled Aggregate | NA: Natural Aggregate.

The mortars (Table 1) were produced in the laboratory using a mechanical mixer and characterized in a fresh and hardened state, 7 samples of each mixture. The consistency index was set at 270mm±20mm according to NBR 13276 (ABNT, 2016). Flexural tensile strength was performed in triplicate on air-cured specimens measuring 40x40x160 mm at 28 days, according to NBR 13279 (ABNT, 2005a). Compressive strength was determined at 28 days on six specimen fragments obtained from the flexural tensile test. The mechanical tests were performed on an Emic Mue 100 model universal machine using a 5-ton cell. The capillarity coefficient was determined according to NBR 15259 (ABNT, 2005b), using 3 specimens for each mixture. The elastic modulus was assessed using the Impulse excitation technique (IET) in three specimens, using the longitudinal method according to E-1876 (ASTM, 2021) and Thomaz, Miyaji and Possan (2021) using an ATCP Physical Engineering nonelastic equipment.

The water retention test was carried out following NBR 13277 (ABNT, 2012). Three specimens were tested for each mixture with the Buncher funnel. Using a vacuum pump, the mortar was subjected to a consistent pressure of 51 mmHg for a duration of 15 minutes. The result was obtained from the ratio between the mass difference of the set before and after suction.

Mortars carbonation

40x40x160mm rendering mortar specimens were exposed to CO₂ natural action for 119 days in three different exposure environments (indoor, outdoor without rain protection, and outdoor with rain protection). Three specimens were submitted to the carbonation test for each studied combination, fractured over time. CO₂ concentrations were monitored automatically during the specimens' exposure time (Figure 2) from an Arduino-based electronic system developed for the study. CO₂, relative humidity, and temperature sensors were attached to the system.

Figure 1 showed that CO₂ concentration was about 492 ppm in the exposure environment, higher than the global annual average (417 ppm) (Stein, 2023). The indoor environment had the highest average concentration as it is a closed laboratory environment without any ventilation. It was noted that CO₂ concentration was higher in the protected environment than in the unprotected one. These environments were near a parking lot, implying high CO₂ exposure throughout the day.

The specimens were fractured longitudinally at each test age to obtain a slice to measure carbonation depth over time. The top of the specimens was not sealed, considering that the CO₂ diffusion rate was not enough to overcome the size of the sample fraction at the test times determined in the experimental design. Carbonation depth measurement was carried out from 14 to 119 days, defined by image analysis using the ImageJ software with the area approximation method for greater accuracy with less operator interference.

CO₂ capture determination by thermogravimetric analysis

For thermogravimetric analysis, specimens exposed for 28 days to the CO₂ natural action outdoors in a rain protection environment were transversely fractured. Phenolphthalein chemical indicator was sprayed on one side of the specimen, as shown in Figure 3. The material was then collected in the mirror specimen (without chemical indicator spray) from the carbonated (C) and non-carbonated (NC) areas. A small aliquot (approximately 5 g) from each area was extracted (Iecron spatula) from a fractured surface of the prismatic specimen after the CO₂ exposure. The collected dry samples were inserted in identified small sample holders, closed, and kept in the laboratory until analyses perform. The sample collection and storage were done carefully to avoid contamination. At first, the collected aliquots were milled, posteriorly sifted on 0.15mm sieves, then stored in hermetically sealed and identified specimen holders and kept in the laboratory until the analysis. This process was carried out quickly to avoid the material's atmospheric carbonation.

Figure 2 - CO₂ concentration over time in different exposure environments collected by Arduino system

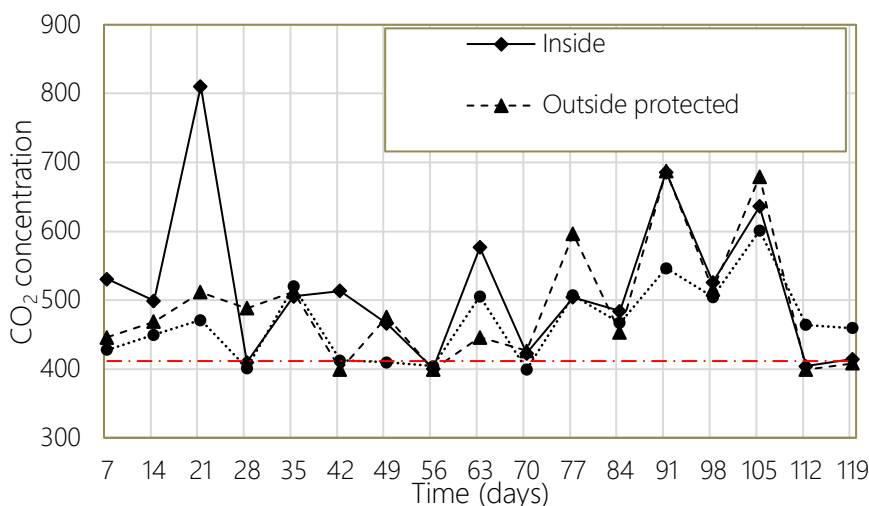
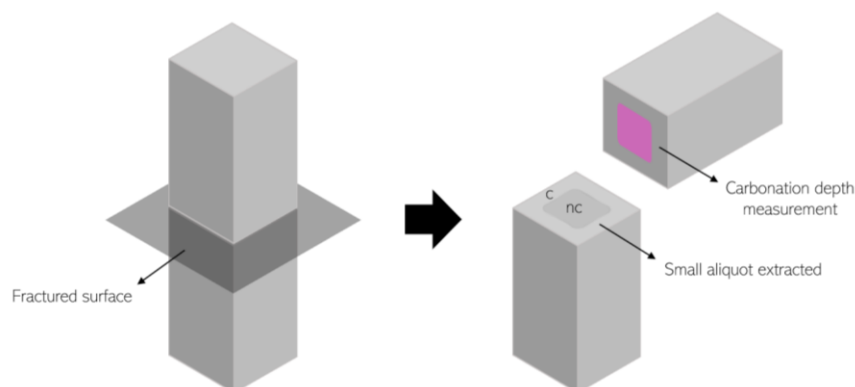


Figure 3 - Sample collection process representation



Thermogravimetric analysis (TGA) was performed using a STA8000 PerkinElmer™ simultaneous thermal analyzer with a reading ranging from 15 to 1600 °C. Alumina crucible, 50±1 mg mass for each specimen, 20 mL.min⁻¹ nitrogen flow, 20 °C.min⁻¹ equipment heating rate and a heating range from 35 °C to 900 °C were used as test parameters. In the first hour of testing, the specimens were preheated inside the equipment at 35 °C for humidity removal. TG and DTG curves were analyzed using the OriginPro® software to determine the CO₂ capture. The compounds' volatilization points from non-carbonated (NC) and carbonated (C) materials and cementitious materials were analyzed to determine the masses corresponding to each characteristic peak's initial and final temperatures. These values were input on tabulation software to calculate the mass loss differences between specimens, as shown in Equations 1 and 2.

$$\%CaCO_3 = (M_{LC} - M_{LNC}) / (M_1) \quad \text{Eq. 1}$$

Where:

%CaCO₃: Present calcium carbonate percentage;

ML_C: Calcium carbonate peak's mass loss from the carbonated sample;

ML_{NC}: Calcium carbonate peak's mass loss from the non-carbonated sample; e

M₁: Calcium carbonate chemical mole fraction.

$$\%MgCO_3 = (M_{LC}) \times (M_2) \quad \text{Eq. 2}$$

Where:

%MgCO₃: Present magnesium carbonate percentage;

ML_C: Magnesium carbonate peaks from the carbonated sample; e

M₂: Magnesium carbonate chemical mole fraction.

Using the tangent method described by Scrivener, Snellings and Lothenbach (2016), it was possible to determine the amount of CO₂ captured between the calcium carbonate, magnesium carbonate molar masses, and carbon dioxide, as seen in Equations 3 and 4.

$$\%CapCO_2 = (\%CaCO_3 \times M_1) + (\%MgCO_3 \times M_2) \quad \text{Eq. 3}$$

Where:

%CapCO₂: Carbon dioxide captured percentage;

%CaCO₃: Present calcium carbonate percentage;

%MgCO₃: Percentage of existing magnesium carbonate; e

M₁ e M₂: Calcium and magnesium carbonate chemical mole fraction, respectively.

$$CapCO_2 = d_1 \times \frac{(\%CaCO_3 + \%MgCO_3)}{m_i \times 0,1} \quad \text{Eq. 4}$$

Where:

CapCO₂: Amount of carbon dioxide captured (kg.CO₂/m³);

d₁: Dry weight (kg/m³);

%CaCO₃: Present calcium carbonate percentage;

%MgCO₃: Present magnesium carbonate percentage; and

m_i: initial sample mass (mg).

Emissions determination

The estimative of CO₂ emissions for mortar production was obtained by the product of the emission adding linked to each material (Table 3) multiplied by consumption (Table 1). The emissions calculation for cement production is mainly due to clinker production by decarbonation and heating of kilns, as well as the use of energy (Equation 5).

$$E = (E_{clinker} \times \%Clinker_{cem}) + (E_{energy} \times EF_{energy}) + E_{filler} \quad \text{Eq. 5}$$

Where:

E_{cem} = Emission for cement production, in kgCO₂/t;

E_{clinker} = Emission for clinker production, in kgCO₂/t;

%Clinker_{cem} = clinker content in cement;

E_{energy} = Emission by electrical energy, in kWh/t;

EF_{energy} = Emission factor of electrical energy, in KgCO₂/kWh; and

E_{filler} = Emission for filler production, in kgCO₂/t.

The clinker content value of cement was obtained by deducting the loss of ignition value (8.05% as per Table 2 and the insoluble residue percentage (12.15%), according to the Cement Test Report, considering a 5% sulfate addition. The cement has a 75% clinker content.

Transport emissions were not included in this study since they depend on the materials manufacturing and the mortar production places, which may vary.

Emission balance

The difference between the total CO₂ emitted (E_{total}) during mortar production and the CO₂ captured by mineralization (Cap_{CO2}) is the emission balance (B_{CO2}), representing the CO₂ captured percentage relative to that emitted (Equation 6).

$$B_{CO2}(\%) = (Cap_{CO2} / E_{total}) \times 100 \quad \text{Eq. 6}$$

Scenarios analysis

As Kaliyavaradhan and Ling (2017) and Possan (2019) proposed, it is possible to determine the potential and effective CO₂ capture due to the mineralization of cement-based materials. Usually, the potential capture does not consider the different material applications expressed in kg. CO₂/m³. The effective or real capture capacity, on the other hand, considers the material during its life cycle, the depth of application, exposure environment, and surface protection, among other factors that affect the CO₂ diffusion in the cement-based material Possan (2019). It is possible to measure CO₂ capture in different scenarios as CO₂ advances over time, which is given by measuring the carbonation depth reaching different ages. With effective capture, it is possible to analyze the behavior of rendering mortar over time by different exposure scenarios analysis, thus forecasting CO₂ capture. In this way, the carbonation depths in the mortar specimens were measured at 14, 28, 42, 63, 91, and 119 days, based on the procedures described by Rilem CPC 18 (1988). Table 4 presents the line equation for each mortar and the mathematical model's respective adjustment coefficient (R²). The line equation was obtained with de values from the 119 fist days carbonation depth.

Table 3 - CO₂ emissions associated with the mortars materials production

Data	Value	Reference
E _{clinker}	832 kg CO ₂ / (1)	GNR Project - Brazil (WBCSD, 2019)
% Clinker _{cem}	75% (2)	NBR 16697 (ABNT, 2013)
E _{energy}	108 kWh/t	GNR Project – Brazil (WBCSD, 2019)
EF _{energy}	0.08 kgCO ₂ /kWh	Ministério da Ciência, Tecnologia e Inovação (MCTIC, 2016)
E _{filler}	8 kgCO ₂ /t	Miller <i>et al.</i> (2018)
E _{lime}	870 kgCO ₂ /t	Tavares and Bragança (2016)
E _{sand}	30 kgCO ₂ /t	Tavares and Bragança (2016)
E _{RA}	5.08 kgCO ₂ /t (3)	Paz <i>et al.</i> (2023)

Note: ¹emissions corresponding to decarbonation and use of fossil fuels in the clinkerization process.

²25% of cement corresponds to carbonate material, pozzolanic addition, and sulfates according to NBR standard.

³the RA of the emission study is the same used on the mortar production.

Table 4 - Linear adjustment of mortar carbonation depth (y) as a function of natural exposure time to CO₂ (x)

Mortar	Linear equation	R ²
0.5L-NA	y= 0.247x-0,1254	0.9664
1.0L-NA	y=0.2092x-0,1379	0.968
2.0L-NA	y=0.1973x-0,2611	0.8736
1.0L-RA	y=0.231x-0,1177	0.9664

For advanced ages, an extrapolation was performed using the Tuutti (1982) model (Equation 7) simulating the carbonated depth that would exceed the 20 mm specimen limit. Equation 7 describes the diffusion of CO₂ in concrete. This was used in this study as a CO₂ diffusion model for rendering mortars was not found in the literature. Because it is not a material with a structural function, the study of CO₂ diffusion in rendering mortars is recent and derived from the current demands for carbon capture due to the carbonation of cement-based materials, which justifies the lack of models. The model was used only in the scenarios study.

$$d_c = k x \sqrt{t} \quad \text{Eq. 7}$$

Where:

d_c = carbonated depth (cm);

k = carbonation coefficient; and

t = time in days.

The CO₂ capture estimative was calculated for the outdoor with rain protection environment, considering the period of six months of natural exposure without surface protection. As shown by Barbosa (2020) surface protection significantly reduces CO₂ capture (up to 38.11% in 164 days).

The determination of scenarios to calculate the masonry amount (m²) that may be coated with 1 m³ of mortar was needed to estimate the capture based on the carbonation depth. The first scenario was determined with an average thickness of 20 mm. From this, it was possible to determine the masonry area that could be coated with 1 m³ of mortar, as shown in Figure 4, resulting in a 50 m²/m³ of mortar ratio. The other scenarios (Table 5) followed the same logic for different depths since different render thicknesses are used due to a lack of control in construction (due to masonry plump correction).

From the thermogravimetric analysis results, it was possible to measure how much CO₂ each mortar captured for each age in kg.CO₂/m³. The surface was considered without any paint or other type of rendering. The CO₂ concentration, relative humidity, and precipitation were not evaluated. For different materials and conditions, other results should be found.

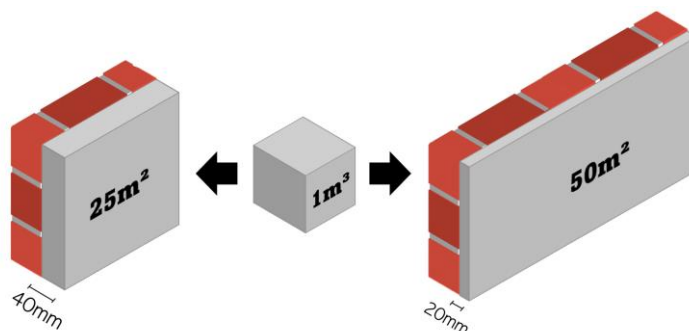
Figure 4 - Schematic representation of the m^2/m^3 ratio

Table 5 - Scenarios description for an outdoor with rain protection environment

Scenario	Renders' thickness (mm)	Surface (m^2/m^3)
1	10.0	100.00
2	20.0	50.00
3	30.0	33.33
4	40.0	25.00
5	50.0	20.00
6	60.0	16.67
7	70.0	14.29
8	80.0	12.50

Results and discussion

Mortars' characterization

Table 6 shows that the mortars used in this study had a low compressive strength for the mortars. However, they are within limits specified by the ABNT 13281 standard (ABNT, 2005c) for rendering mortars, meeting the density, workability, capillarity, resistance, and compatibility standards for the application surface.

A similar consistency index of the mortars was maintained, between 270 ± 20 , varying the water consumption (Table 1). The higher the lime content, the greater the water retention and the greater the amount of water needed to achieve the desired consistency Chever, Pavía and Howard (2010). The mortars' performance in the fresh and hardened state must be observed since adding RA at certain ratios may reduce mortars' flexural tensile strength and compressive strength (Mazurana *et al.*, 2021). Andrade *et al.* (2018) observed that the higher the RA contents in the mortar composition, the greater the porosity and water absorption (Table 2), and the lower the density and mechanical resistance. According to the literature, such a decrease is directly related to the increase in the amount of water required to achieve workability, leading to a greater material porosity in the hardened state. Porosity is linked to an increase in water consumption and a decrease in cement content. It is observed that the 1.0L-RA mortar presented similar behavior to 2.0L-NA for such characteristics. Replacing NA for RA by up to 30% gives a satisfactory performance in the fresh and hardened state to produce rendering mortars (Andrade; Sanjuán, 2018; Muñoz-Ruiperez *et al.*, 2016). The higher the lime content, the lower the flexural tensile strength and the lower the stiffness. The increase in lime content has a negative influence on the compressive strength due to the lower cement content and the greater water retention since cement is the main responsible for the strength development. No correlation was found in this study between the lime and RA content in these properties. For the elasticity modulus, it was observed that the higher the lime content, the lower the stiffness. The replacement of 25% of NA by RA increase only 3% on this property.

Mortar carbonation

According to Pauletti, Dal Molin and Possan (2007), the diffusion of CO_2 is hindered in unprotected outdoor environments that are subject to rain, whereas indoor environments promote faster carbonation due to better control and facilitation of CO_2 diffusion. The environments that most contributed to the increase of the carbonation degree were the outdoor with rain protection environment, followed by the outdoor without rain protection environment, mainly in the early stages of exposure, as seen in Figures 1 and 5. Such an occurrence may be due to the specific characteristics of each environment.

Figure 5 shows that the carbonation depth increased over time in all environments studied. This was due to the CO₂ diffusion into the mortar pores, allowing the carbonation reaction to occur. It was noted that the ambient with the highest carbonation depth values was primarily the protected outdoor ambient, followed by the unprotected indoor ambient and the indoor ambient, indicating the relative humidity and CO₂ concentration influence on the carbonation front. For mortars with NA at the indoor ambient, the lower the lime content, the greater the carbonation depth, as shown in Figure 5. This may be attributed to mortars with higher lime content and thus higher alkaline reserve. Since they have greater amounts of calcium hydroxide and magnesium hydroxide available for chemical reaction with CO₂, it slows down the carbonation front Mazurana *et al.*, (2021). The carbonation depth increased by replacing NA for RA, corroborating the results of Andrade *et al.* (2018). The RA can lead to an increase in carbonation coefficient K (Leemann; Loser, 2019). This was directly related to RA's porosity, which facilitated CO₂ diffusion and, consequently, the carbonation reactions (Han; Jun; Kim, 2023; Leemann; Loser, 2019; Mazurana *et al.*, 2021).

CO₂ capture

Figures 6 and 7 show the TGA curves of the carbonated (C) and non-carbonated (NC) areas for the mortars studied. It was noticed that the mass loss occurred in three distinct stages, and the residual mass varied according to each sample. A lower residual mass was observed for the carbonated samples than for the non-carbonated ones. Carbonated mortars region (C) showed a greater mass loss at temperatures ranging between 650 °C and 800 °C (Peak 3) than the non-carbonated mortars region (NC). This happened due to the increased calcium carbonate concentration through the mortar carbonation process, where calcium hydroxide reacted with CO₂ and precipitated as calcium carbonate (Xuan; Zhan; Poon, 2016).

It can be noticed a small carbonation depth from the 2.0L-NA due to the greater alkaline reserve, which diminishes the CO₂ diffusion. The TGA curves (Figure 6) indicate a high carbon fixation result (mineralization) which will be higher with an increase in the alkaline reserve, indicating a more conversion of hydroxides into carbonates. In matrices with higher alkaline reserves, the carbonation depth is small, but the carbon fixation is high.

For the non-carbonated mortars, peak 1 was attributed to water loss from the magnesium hydroxide (Mg(OH)₂) decomposition in lime at temperatures between 360 °C and 450 °C. For the carbonated specimens, magnesium carbonate decomposition (peak 4) occurred in the same temperature range (Mazurana *et al.*, 2021). Peak 2 (between 400 °C and 500 °C) was attributed to the calcium hydroxide decomposition, which is less in the carbonated mortars since it reacted with CO₂ during mineralization to form calcium carbonate (CaCO₃). Peak 2 intensity was higher for non-carbonated samples due to the higher amount of free hydroxides in the matrix (calcium and magnesium) since the carbonation reaction did not occur. The last and highest peak (peak 3) occurred above 650 °C. It was attributed to the calcium carbonate decomposition formed by the chemical reaction of carbonation where calcium hydroxide reacted with CO₂ or is from the limestone filler added to the Portland cement production used in the mortar (Li *et al.*, 2018; Neves Junior *et al.*, 2019).

Table 6 - Mortars in fresh and hardened state characterization

Mortar	Fresh state test			Hardened state test		
	Consistency index (mm)	H ₂ O retention (%)	Flexural strength (MPa)	Compressive strength (MPa)	Capillary H ₂ O Absorption (g/dm ² .min ^{1/2})	Elastic modulus (GPa)
0.5L-NA	258	58.3	0.86	2.40	18.80	6.19
1.0L-NA	252	68.8	0.63	1.60	24.58	4.14
2.0L-NA	247	85.9	0.57	1.70	20.07	3.79
1.0L-RA	251	88.3	0.78	1.79	20.21	4.27

Figure 5 - Depth carbonation for different environments

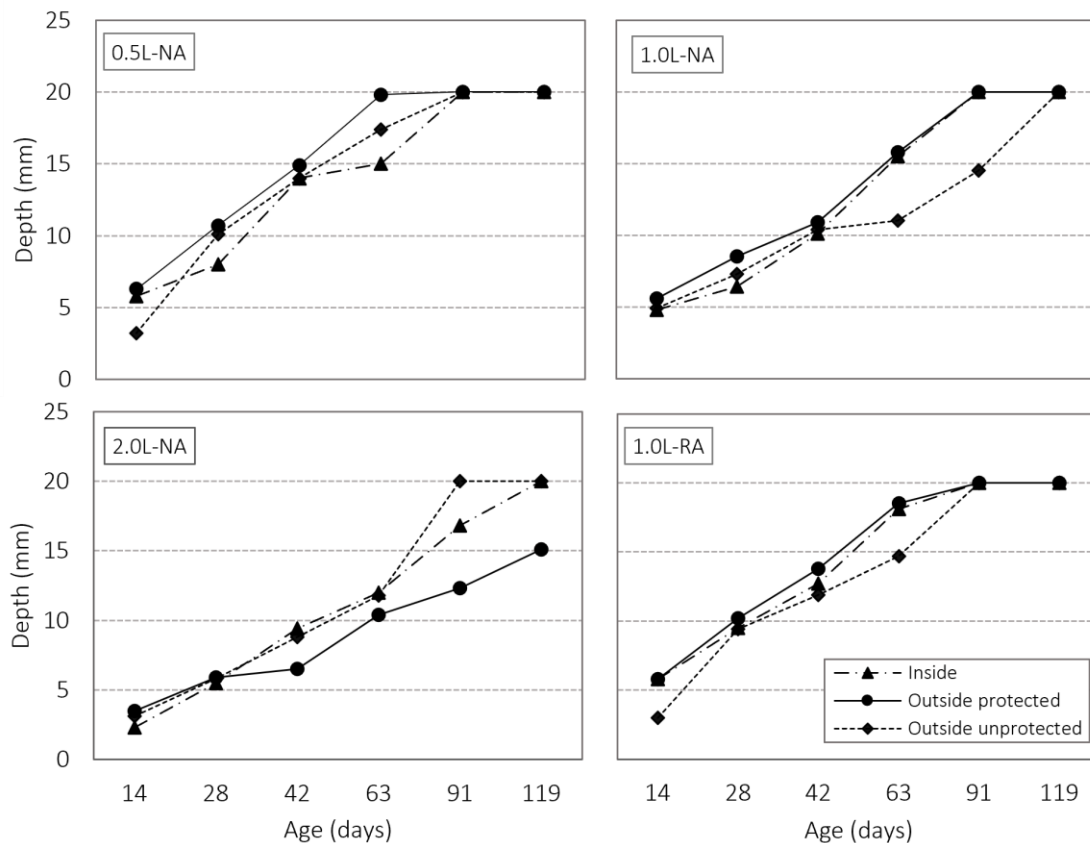


Figure 6 - carbonated (c) and non-carbonated (nc) mortars' TGs Curves

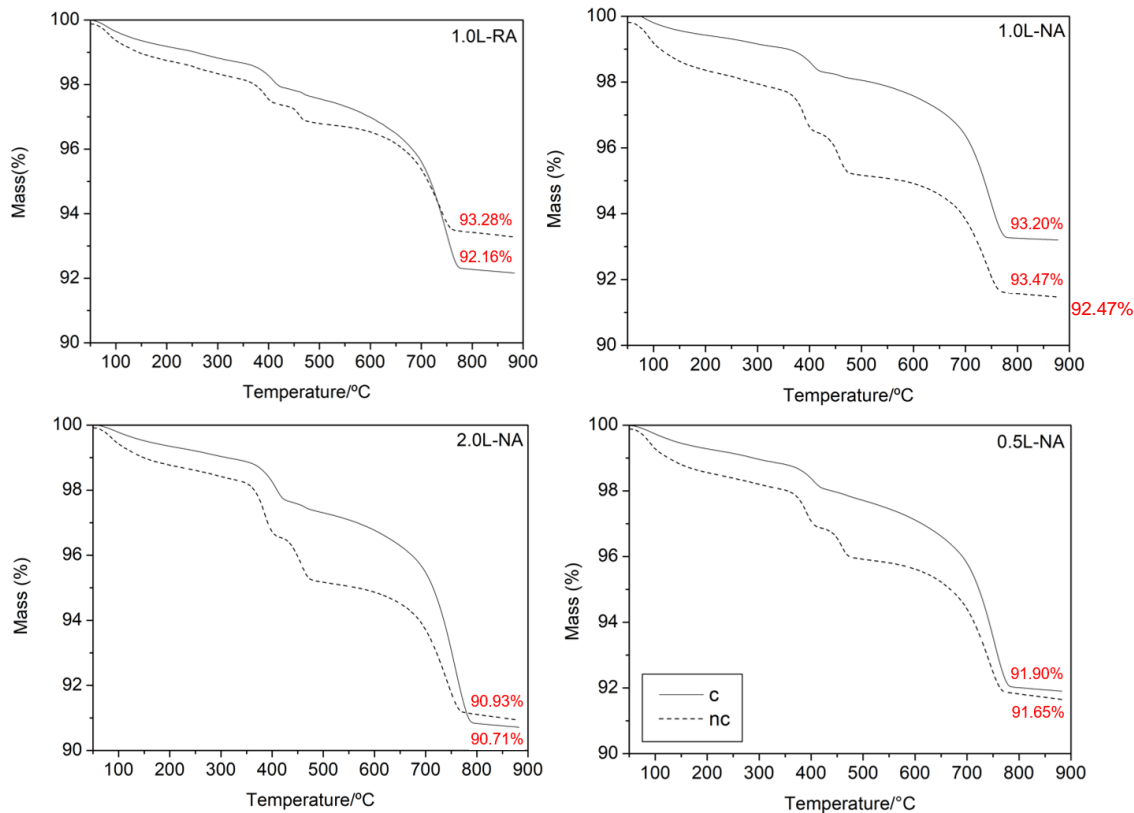


Figure 7 - carbonated (c) and non-carbonated (nc) mortars' DTGs

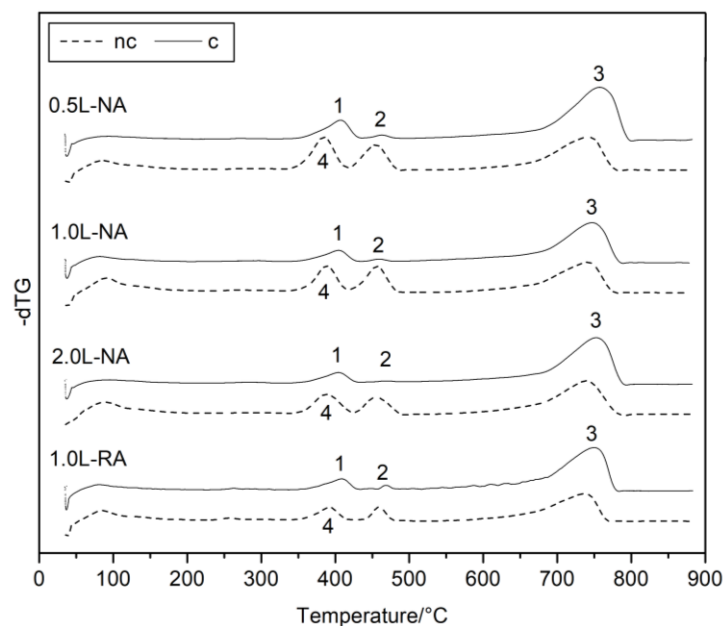


Figure 6 shows that the 1.0L-RA specimen had a higher mass loss and a higher peak from 650 °C to 800 °C. Peak 4 increased in the carbonated specimens with RA content, showing a higher amount of calcium carbonate to be decomposed beyond magnesium carbonate; the higher the RA addition, the higher the amount of the carbonates (Cai; Wang; Xiao, 2018; Kaliyavaradhan; Ling, 2017). This occurred as the RA was already carbonated, as shown in Figure 8, and due to the higher porosity when recycled aggregates are used. While the natural aggregate presented 1.20% absorption, the recycled sand presented 10.48%, facilitating CO₂ diffusion. The RA was partially carbonated, with the release of adsorbed CO₂ at 250 °C and the release of combined CO₂ at 750 °C. The pre-carbonation of recycled aggregates comes from their use as a building material. It can come from the carbonation reactions of the recycled aggregate with the ambient CO₂ from its production to its use (El-Dieb; Kanaan, 2018; Kaliyavaradhan; Ling, 2017; Ruviano et al., 2022).

When analyzing the non-carbonated specimens produced with RA (Figure 7), minor peaks in the derivative curves at temperatures ranging from 250 °C to 750 °C were noted, evidencing this conclusion. In addition, prominent peaks were noticed for hydrated lime, which, as it was a magnesium lime, released magnesium and calcium hydroxide, resulting in a mass loss (30.94%) higher than cement (7.67%) and RA (10.42%).

Using the tangent method, the CO₂ captured values (Table 7) by the samples under study were calculated due to natural exposure to CO₂ (Equations 3 and 4). It was noted (Table 7) that the higher the hydrated lime content, the higher the potential of CO₂ capture. This was due to the amount of carbonatable materials available in the matrix. In cement-lime mortars, calcium hydroxide comes from Portland cement's hydration process and calcium and magnesium hydroxides are present in hydrated lime. These products chemically react with carbon dioxide forming stable calcium and magnesium carbonates (Mo; Panesar, 2013). For CO₂ diffuses into the mortar, it must react with Ca(OH)₂ and Mg(OH)₂, so the amount of CO₂ captured inside the lime-based mortars may be higher by increasing lime content (Mazurana et al., 2021).

For specimens with and without RA and the same 25% hydrated lime content, using RA increased the potential of CO₂ capture by 6%. The increase of CO₂ capture using RA content may be observed when comparing the mortar of the same rate with 100% natural aggregate (1.0L-RA and 1.0L-NA). Replacing NA for RA makes more cementitious materials available and, consequently, calcium hydroxide for carbonation, which favors CO₂ sequestration from the environment, as verified by Andrade et al. (2018). For TGA analysis, the maximum amount of CO₂ captured was observed in the mortar with the highest lime content (2.0L-NA), 25.41 Kg CO₂/m³, and the minimum capture was 15.97 Kg CO₂/m³ for mortar with the lowest lime content (0.5L-NA).

Figure 9 shows the specimen characterization divided into two groups. The first one compared specimens of NA with different lime contents (0.5L-NA, 1.0L-NA, and 2.0L-NA) (Figures 9a and 9c), and the second one compared the same lime content but varying the RA content (1.0L-RA and 1.0L-NA) (Figure 9b).

Figure 9c shows that increasing the amount of lime in the mortar's ratio increased the water retention and thus CO₂ capture. However, capillarity increased only up to the binders (cement: lime) 1:1 ratio; when the lime content doubled from 1 to 2 in the mixture, capillarity decreased by 18.35%. This was an interesting result as it reduced the possibility of water entering lime- based render (Carasek, 2010).

Figure 8 - (a)thermogram and (b) DTG curve for mortar materials production

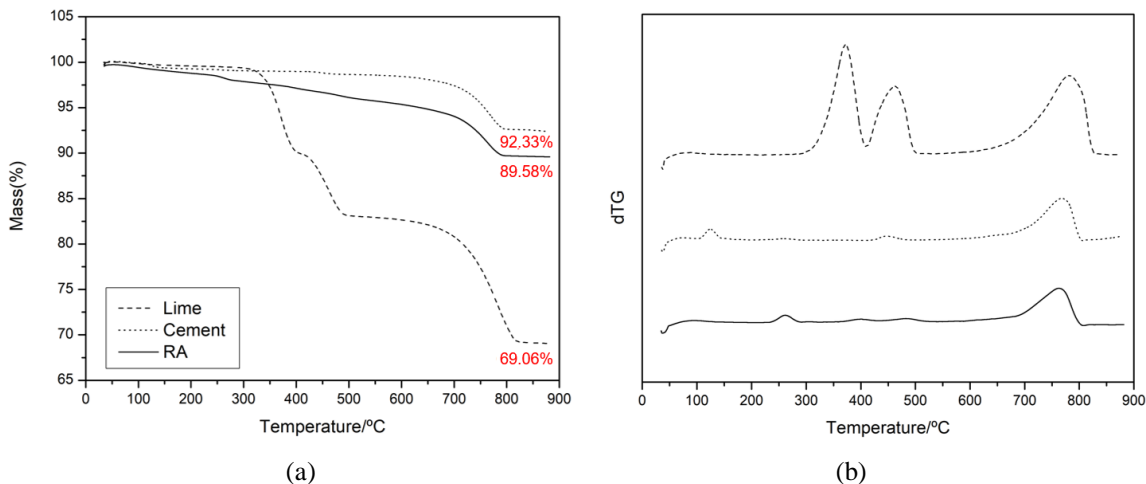
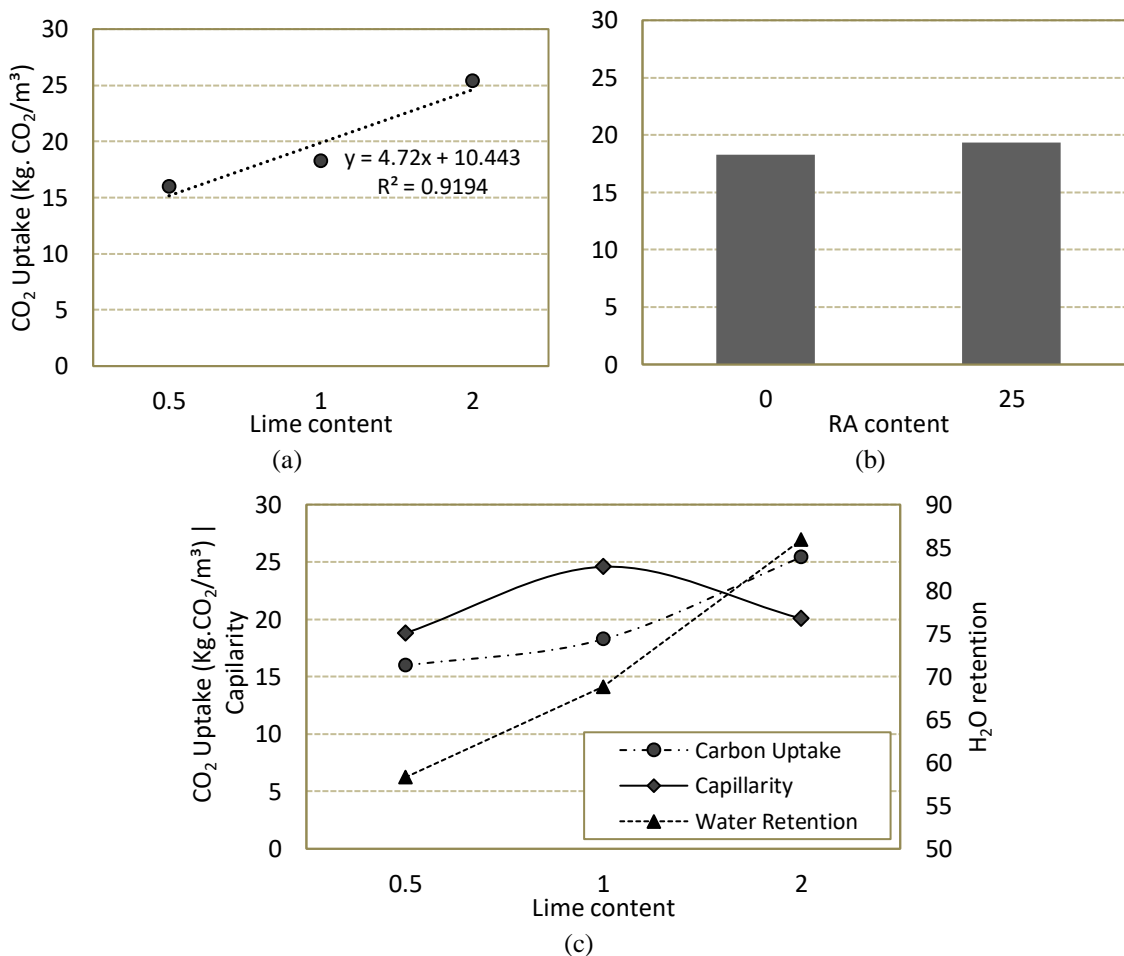


Figure 9 - Mortars characterization according to (a) the lime content, (b) the RA content for the same lime content, and (c) properties



Replacing NA for RA in the mixture increased carbon dioxide capture capacity, as the second one has a non-hydrated binder in its composition, which enhances carbonation. Also, increasing the amount of lime added to the mixture increased CO₂ capture since the higher the amount of binder, the higher the potential for mortar mineralization.

CO₂ emissions

For CO₂ emissions associated with rendering mortar production, it was noted that they were directly proportional to the hydrated lime content used (Figure 9). Hydrated lime was the material with the highest influence on emissions, followed by Portland cement. John, Punhagui and Cincotto (2014) stated that this is due to the lime production process in Brazil. As a heterogeneous sector, there are variations in the size and quality of companies and product technology. The CO₂ emissions of lime production come from limestone decarbonation inherent to the process and from burning fuels in the manufacturing process. The lack of efficiency and control of kilns and the applied technologies influence the type and amount of fuel consumed, which are directly related to the energy consumed by the sector and CO₂ emissions.

Figure 10 shows that the mortar with the highest emission (2.0L-NA) had the highest binder consumption as it was primarily responsible for the CO₂ emitted during the mortar production process. The less emissive mortar was the 0.5L-NA, with 211.15 KgCO₂/m³, 36.55% lower than the higher emissive one (2.0L-NA, with 332.78 KgCO₂/m³). Hydrated lime is an essential component in rendering mortars as it improves plasticity and water retention, as seen in Figure 9. It has a lower cost and easier production than Portland cement and is widely available in Brazil.

A global analysis that considers the properties in the fresh and hardened state, emissions, and CO₂ capture is important to establish the optimal content of this material for mortar production. Natural aggregate replaced by recycled aggregate reduced emissions by 7.28% compared to the mortar with NA and the same lime ratio. Using RA in the 1.0L-RA mixture reduced up to 29.1% of the emissions compared to the other ratios, as the emissions for recycled aggregate production were about 83% lower than those of the natural aggregate. The RA carbon footprint can differ depending on the recycling process adopted. The RA used in this study received only mechanical processing, resulting in lower emissions when compared to NA. With other associated RA treatment processes, such as Jigging (Malysz *et al.*, 2022) coating with pozzolan slurry (Al-Waked *et al.*, 2022), mechanical (Oliveira; Dezen; Possan, 2020; Wang; Mu; Liu, 2018), thermal (El-Dieb; Kanaan, 2018) and chemical treatments such as tannic acid (Fang *et al.*, 2022; Wang *et al.*, 2022), the carbon footprint may be higher. Knowing the RA production process for emission studies is central (Infante Gomes *et al.*, 2021).

CO₂ emissions balance

Table 8 showed that the mortar with the best performance in reducing CO₂ emissions was the one at the 1:1:6 ratio with 25% RA replacement, capturing approximately 8.15% of the CO₂ emitted during mortar production. This was followed by the 1:2:6 ratio mortar with 0% RA, which captured up to 7.64%. It is essential to evaluate the emissions balance to understand the behavior between emission and capture. As the materials used in mortar production usually have different carbon footprints, these may not be offset only by capture due to mineralization. Lime-based mortars had higher CO₂ emissions. However, its CO₂ capture was also higher so the decrease in the use of the binder decreased the final balance. The use of RA collaborated positively with the final emissions balance, as this aggregate emitted less CO₂ during the production process when compared to natural aggregate (Mazurana *et al.*, 2021) and part of it gets in the mixture already pre-carbonated mixture. The amount of CO₂ uptake increased with the increasing replacement of natural sand with recycled sand and with increasing lime. As well as reducing emissions, the replacement of natural sand with RA aggregate also increased CO₂ capture, making RA mortar production clearly beneficial.

Scenarios analysis

Figure 11 shows the CO₂ capture results, obtained by thermal analysis (Table 7), over time in the various scenarios studied. The TGA results were multiplied by the advance of CO₂ over time (Equations 4 and 7), which is given by the projection of the carbonation front.

Figure 10 - Emissions from 1m³ of mortar production per material

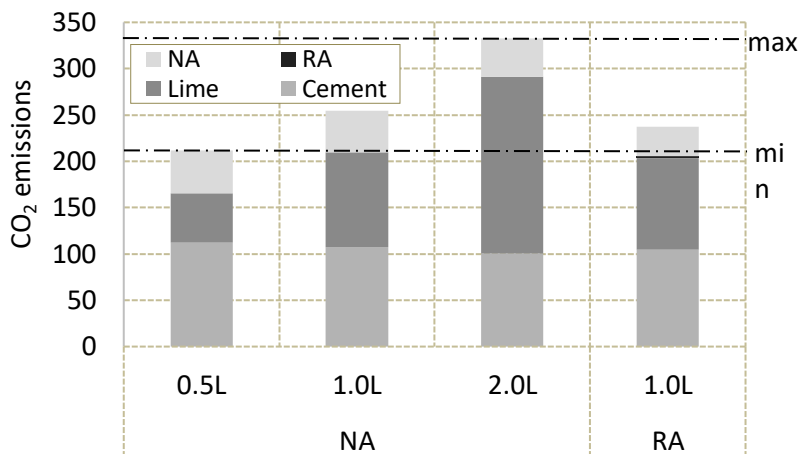


Table 8 - CO₂ balance emissions

Mortar	Capture (kg.CO ₂ /m ³)	Emission (Kg.CO ₂ /m ³)	Balance (Kg.CO ₂ /m ³)	Balance (%)
0.5L-NA	15.97	211.68	195.71	7.55
1.0L-NA	18.27	254.49	236.22	7.18
2.0L-NA	25.41	332.78	307.37	7.64
1.0L-RA	19.37	237.63	218.26	8.15

Figure 11 - Effective CO₂ capture over time considering the mortar type and depth

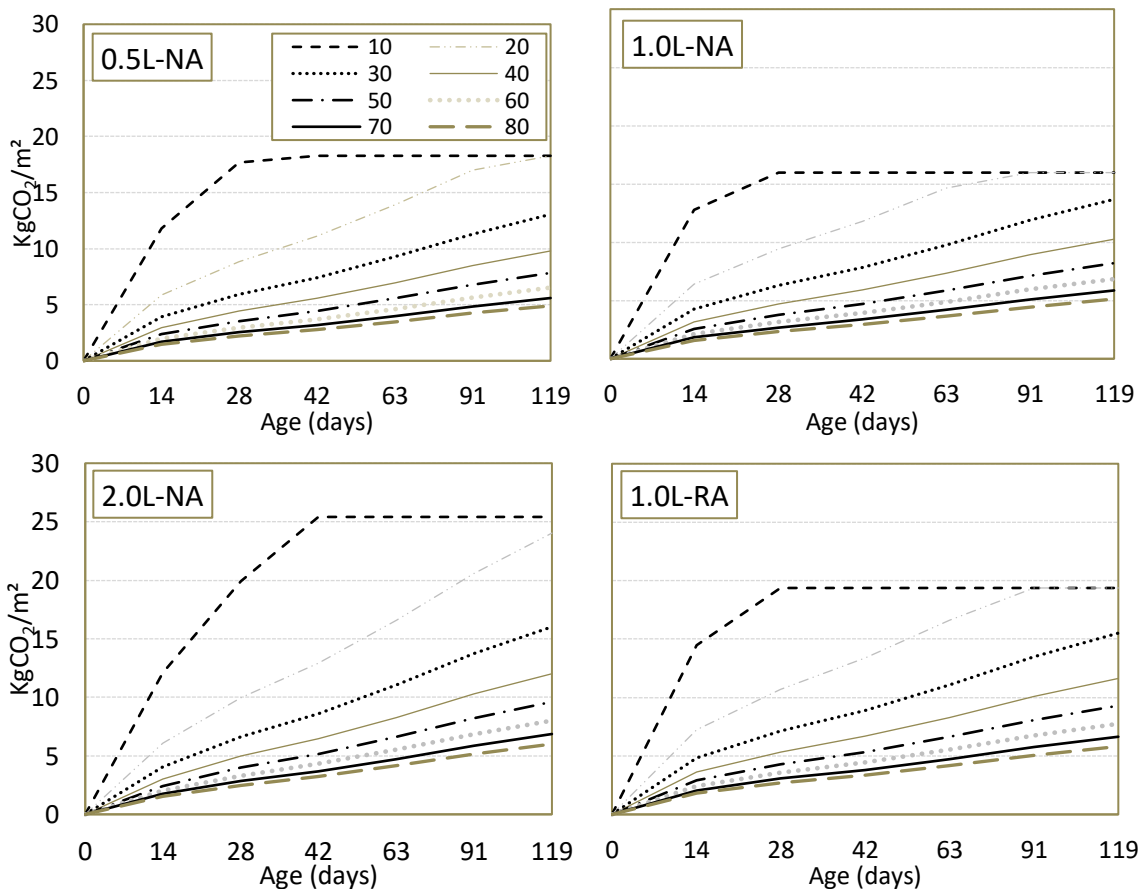


Table 9 - Best time needed for total carbonation in days

Depth (mm)	0.5L-NA	1.0L-NA	2.0L-NA	1.0L-RA
10	28	28	42	28
20	91	119	147	91
30	182	365 (1 year)	365 (1 year)	182
40	365 (1 year)	547 (1.5 years)	547 (1.5 years)	365 (1 year)
50	547 (1.5 years)	730 (2 years)	730 (2 years)	547 (1.5 years)
60	730 (2 years)	912 (2.5 years)	1095 (3 years)	730 (2 years)
70	912 (2.5 years)	1460 (4 years)	1460 (4 years)	1095 (3 years)
80	1095 (3 years)	1825 (5 years)	1825 (5 years)	1460 (4 years)

Figure 11 shows that the maximum CO₂ captured was achieved in short periods at lower render thicknesses, with carbon capture occurring until the carbonated depth is equal to the render thickness. Higher surface area results in greater carbonation depths because it promotes CO₂ diffusion. The potential of CO₂ capturing was achieved by carbonation completion. 10 mm-thick renderings in direct contact with CO₂ for short periods before receiving a finishing layer (paint, ceramic, etc.) will certainly reach their maximum potential of CO₂ capture. Figure 5 shows that the maximum CO₂ penetration depth into the material was 10.7 mm after 28 days of exposure. Considering the rendering mortar application thickness without a surface layer and its CO₂ diffusion capacity over time, later exposure ages generate a higher amount of CO₂ capture.

Table 9 shows that thicknesses higher than 20 mm require time exposure to CO₂ for more than 3 months for complete carbonation and maximum carbon fixation. The time required for complete material carbonation increases exponentially as the thickness increases, not considering the surface protection effect. Barbosa (2020) stated that CO₂ diffusion in mortars is 3 times smaller when wall painting, affecting carbon capture capacity.

For render thicknesses higher than 30 mm, the time for CO₂ diffusion and complete carbonation of the material used in construction is 1 to 4 years, depending on the mortar composition. Thicknesses more than 50 mm, take 4 to 20 times longer to reach maximum carbonation when compared to smaller ones (20 mm).

A six-month exposure period was insufficient for all mortars thicker than 20 mm to reach their maximum carbonation depth and, consequently, their potential CO₂ capture. A longer period in direct contact with CO₂ before receiving a layer was required for complete carbonation. However, mortar may reach maximum potential CO₂ capture in buildings exposed to the wall for long periods.

Renders thicker than 20 mm, resulting from poor quality control and construction execution, increase CO₂ emissions, and the construction cost per m² should be avoided.

Although RA cost is lower than natural aggregate, there is still resistance to using this waste due to limited knowledge of cement-based applications. In this way, it is deemed necessary to motivate the use of RA through public policies, which act not only to encourage its use but also in investment and research dissemination.

It highlights the importance of studying CO₂ capture in cement-based mortars and the influence of lime and RA, as they may balance part of the emissions generated by the building materials production process.

Conclusions

This work presents the results of CO₂ capture from different scenarios of mortar applications, obtained by natural carbonation. In the circular economy and the cleaner production context, the natural aggregate (NA) was replaced by recycled aggregate (RA) and three different hydrated lime contents were evaluated.

- the results indicated that the carbonation process in rendering mortars was significant in CO₂ uptake, and the thermogravimetric analysis method proved to be effective in calculating carbon fixation;
- the mortars studied could neutralize between 7.18 and 8.15% of CO₂ emitted during their production, depending on the presence or absence of hydrated lime and the amount of RA used in their production;
- mortars presented a high potential for CO₂ capture with increasing lime content. The maximum amount of CO₂ captured occurred in the 2.0L-NA mortar, 25.41 Kg CO₂/m³ at 28 days. For specimens added with RA or not and the same hydrated lime content, using 25% of RA increased the potential for CO₂ capture by 6%;

- (d) the mortar with the highest emissions was 2.0L-NA (336.78 Kg CO₂/m³) due to the high lime content and natural aggregate. High binder levels and the exclusive use of natural aggregates were indeed responsible for increasing the final emissions value;
- (e) the production of mortars with RA benefits the CO₂ balance and reduces the use of natural resources. For the same lime content, natural sand replaced by RA reduced emissions (254.49 to 237.63 Kg CO₂/m³) and increased CO₂ capture (18.27 to 19.37 Kg CO₂/m³);
- (f) the rendering mortar thickness, the type of mortar, and the exposure time to CO₂ before applying the finish surface layer affect the carbon capture result. The higher the lime content, the lower the CO₂ diffusion speed and the higher the carbon fixation in the rendering mortar;
- (g) the m²/m³ ratio is directly proportional to the carbon fixation in the lime-cement-based matrix. The higher this ratio, the shorter the time for the material to be fully carbonated and, consequently, to end the CO₂ capture potential. Thicknesses higher than 20 mm required exposure to CO₂ for more than 3 months for complete carbonation and maximum carbon fixation. Thicknesses higher than 50 mm took 4 to 20 times longer to reach maximum carbonation when compared to the 20 mm; and
- (h) it appears that the rendering mortar thickness application control ensured a lower amount of material used per m², avoiding incorporated losses and an impact on emissions and CO₂ capture.

Reference

- AL-WAKED, Q. *et al.* Enhancing the aggregate impact value and water absorption of demolition waste coarse aggregates with various treatment methods. **Case Studies in Construction Materials**, v. 17, p. e01267, 2022.
- AMERICAN SOCIETY FOR TESTING AND MATERIALS. **E-1876**: standard test method for dynamic young's modulus, shear modulus, and poisson's ratio by impulse excitation of vibration. Philadelphia, 2021.
- ANDRADE, C.; SANJUÁN, M. Updating carbon storage capacity of spanish cements. **Sustainability**, v. 10, n. 12, p. 4806, 2018.
- ANDRADE, J. J. O. *et al.* Evaluation of mechanical properties and carbonation of mortars produced with construction and demolition waste. **Construction and Building Materials**, v. 161, 2018.
- ASSOCIAÇÃO BRASILEIRA DE NORMAS TÉCNICAS. **NBR 13276**: mortars applied on walls and ceilings: determination of the consistence index. Rio de Janeiro, 2016.
- ASSOCIAÇÃO BRASILEIRA DE NORMAS TÉCNICAS. **NBR 13277**: argamassa para assentamento e revestimento de paredes e tetos: determinação da retenção de água. Rio de Janeiro, 2012.
- ASSOCIAÇÃO BRASILEIRA DE NORMAS TÉCNICAS. **NBR 13279**: argamassa para assentamento e revestimento de paredes e tetos: determinação da resistência à tração na flexão e à compressão. Rio de Janeiro, 2005a.
- ASSOCIAÇÃO BRASILEIRA DE NORMAS TÉCNICAS. **NBR 13281**: argamassa para assentamento e revestimento de paredes e tetos: requisitos. Rio de Janeiro, 2005c.
- ASSOCIAÇÃO BRASILEIRA DE NORMAS TÉCNICAS. **NBR 15259**: argamassa para assentamento e revestimento de paredes e tetos: determinação da absorção de água por capilaridade e do coeficiente de capilaridade. Rio de Janeiro. 2005b.
- ASSOCIAÇÃO BRASILEIRA DE NORMAS TÉCNICAS. **NBR 16697**: revestimento de paredes e tetos de argamassas inorgânicas: especificação. Rio de Janeiro, 2013.
- BARBOSA, M. C. **Efeito da proteção superficial do tipo pintura na captura de CO₂ por carbonatação em argamassas de revestimento**. Curitiba, 2020. Dissertação (Mestrado em Engenharia Civil) – Universidade Tecnológica Federal do Paraná, Curitiba, 2020.
- BORGES, P. M. *et al.* Mortars with recycled aggregate of construction and demolition waste: mechanical properties and carbon uptake. **Construction and Building Materials**, v. 387, 2023.
- CAI, J.; WANG, S.; XIAO, Z. A study on the CO₂ capture and attrition performance of construction and demolition waste. **Fuel**, v. 222, p. 232–242, 2018.
- CARASEK, H. Argamassas. In: ISAIA, G. C. (org.). **Materiais de construção civil e princípios de ciência e engenharia de materiais**. São Paulo: IBRACON, 2010.

- CHEVER, L.; PAVÍA, S.; HOWARD, R. Physical properties of magnesian lime mortars. **Materials and Structures**, v. 43, n. 1–2, p. 283–296, 2010.
- COPPOLA, L. *et al.* An Empathetic Added Sustainability Index (EASI) for cementitious based construction materials. **Journal of Cleaner Production**, v. 220, p. 475–482, 2019.
- COSTA, F. N.; RIBEIRO, D. V. Reduction in CO₂ emissions during production of cement, with partial replacement of traditional raw materials by civil construction waste (CCW). **Journal of Cleaner Production**, v. 276, p. 123302, 2020.
- DELABONA, F. J.; GAVA, G. P.; RUFATTO, M. Avaliação do potencial de captura de CO₂ em argamassas de revestimento devido à carbonatação natural. In: ENCONTRO ANUAL DE INICIAÇÃO CIENTÍFICA, 6., Cascavel, 2020. **Anais [...]** Cascavel, 2020.
- EL-DIEB, A. S.; KANAAN, D. M. Ceramic waste powder an alternative cement replacement: characterization and evaluation. **Sustainable Materials and Technologies**, v. 17, p. e00063, 2018.
- ERGENÇ, D.; FORT, R. Accelerating carbonation in lime-based mortar in high CO₂ environments. **Construction and Building Materials**, v. 188, p. 314–325, 2018.
- FANG, Y. *et al.* A renewable admixture to enhance the performance of cement mortars through a pre-hydration method. **Journal of Cleaner Production**, v. 332, p. 130095, 2022.
- FONTOLAN, B. L.; GAVA, G. P.; SILVA, T. B. Contribuição ao sequestro de CO₂ devido a carbonatação natural de argamassas com agregado de resíduo de construção e demolição. In: ENCONTRO ANUAL DE INICIAÇÃO CIENTÍFICA, 6., Cascavel, 2020. **Anais [...]** Cascavel, 2020.
- FORSTER, A. M. *et al.* Lime binders for the repair of historic buildings: Considerations for CO₂ abatement. **Journal of Cleaner Production**, v. 252, p. 119802, 2020.
- FUKUI, E. *et al.* CO₂ liberado na produção de argamassas. In: SIMPÓSIO BRASILEIRO DE TECNOLOGIA DAS ARGAMASSA, 10., Fortaleza, 2013. **Anais [...]** Fortaleza, 2013.
- HAN, S. H.; JUN, Y.; KIM, J. H. The use of monoethanolamine CO₂ solvent for the CO₂ curing of cement-based materials. **Sustainable Materials and Technologies**, v. 35, p. e00559, 2023.
- INTERNATIONAL ENERGY AGENCY; WORLD BUSINESS COUNCIL FOR SUSTAINABLE DEVELOPMENT. **Technology Roadmap: Low-Carbon Transition in the Cement Industry**. Paris, 2018.
- INFANTE GOMES, R. *et al.* CO₂ sequestration by construction and demolition waste aggregates and effect on mortars and concrete performance: an overview. **Renewable and Sustainable Energy Reviews**, v. 152, p. 111668, 2021.
- INTERGOVERNMENTAL PANEL ON CLIMATE CHANGE. **Climate change 2021: the physical science basis**. contribution of working group I to the sixth assessment report of the IPCC. New York: Cambridge University Press, 2021.
- JOHN, V. M.; PUNHAGUI, K. R. G.; CINCOTTO, M. A. **Produção de cal: economia de baixo carbono, impactos de novos marcos regulatórios e tecnologias sobre a economia brasileira**. Ribeirão Preto: Funpec, 2014.
- KALIYAVARADHAN, S. K.; LING, T.-C. Potential of CO₂ sequestration through construction and demolition (C&D) waste: an overview. **Journal of CO₂ Utilization**, v. 20, p. 234–242, 2017.
- KANG, S.-H.; KWON, Y.-H.; MOON, J. Quantitative analysis of CO₂ uptake and mechanical properties of air lime-based materials. **Energies**, v. 12, n. 15, p. 2903, 2019.
- LEEMANN, A.; LOSER, R. Carbonation resistance of recycled aggregate concrete. **Construction and Building Materials**, v. 204, p. 335–341, 2019.
- LI, D. *et al.* Evaluating the effect of external and internal factors on carbonation of existing concrete building structures. **Construction and Building Materials**, v. 167, p. 73–81, 2018.
- MADDALENA, R.; ROBERTS, J. J.; HAMILTON, A. Can Portland cement be replaced by low-carbon alternative materials? A study on the thermal properties and carbon emissions of innovative cements. **Journal of Cleaner Production**, v. 186, p. 933–942, 2018.
- MALYSZ, G. N. *e al.* Natural and accelerated carbonation in concrete associated with recycled coarse aggregate treated by air jiggling technology. **Journal of Materials in Civil Engineering**, v. 34, n. 7, 2022.

- MAZURANA, L. *et al.* Determination of CO₂ capture in rendering mortars produced with recycled construction and demolition waste by thermogravimetry. **Journal of Thermal Analysis and Calorimetry**, v. 147, p. 1071-1080, jan. 2021.
- MILLER, S. A. *et al.* Carbon dioxide reduction potential in the global cement industry by 2050. **Cement and Concrete Research**, v. 114, p. 115–124, 2018.
- MO, L.; PANESAR, D. K. Accelerated carbonation: a potential approach to sequester CO₂ in cement paste containing slag and reactive MgO. **Cement and Concrete Composites**, v. 43, p. 69–77, 2013.
- MUÑOZ-RUIPEREZ, C. *et al.* Lightweight masonry mortars made with expanded clay and recycled aggregates. **Construction and Building Materials**, v. 118, p. 139–145, 2016.
- NEVES JUNIOR, A. *et al.* Determination of CO₂ capture during accelerated carbonation of engineered cementitious composite pastes by thermogravimetry. **Journal of Thermal Analysis and Calorimetry**, v. 138, n. 1, p. 97–109, 2019.
- OLIVEIRA, T. C. F.; DEZEN, B. G. S.; POSSAN, E. Use of concrete fine fraction waste as a replacement of Portland cement. **Journal of Cleaner Production**, v. 273, p. 123126, 2020.
- PAULETTI, C.; DAL MOLIN, D. C. C. D.; POSSAN, E. Accelerated carbonation: state-of-the art of the research in Brazil. **Ambiente Construído**, Porto Alegre, v. 7, n. 4, p. 7–20, out./dez. 2007.
- PAZ, C. F. *et al.* Life cycle inventory of recycled aggregates derived from construction and demolition waste. **Journal of Material Cycles and Waste Management**, v. 25, n. 2, p. 1082–1095, 2023.
- POSSAN, E. Captura de CO₂ em materiais cimentícios. **Concreto & Construção**, v. 1, p. 60–66, 2019.
- PUNHAGUI, K. R. G. *et al.* **Estudo de baixo carbono para a indústria de cimento no estado de São Paulo de 2014 a 2030: sumário executivo**. São Paulo: CETESB, 2018. v. 1.
- RILEM. CPC-18: measurement of hardened concrete carbonation depth. **Materials and Structures**, v. 21, n. 6, p. 453–455, 1988.
- RUVIARO, A. S. *et al.* Long-term effect of recycled aggregate on microstructure, mechanical properties, and CO₂ sequestration of rendering mortars. **Construction and Building Materials**, v. 321, p. 126357, 2022.
- ŠAVIJA, B.; LUKOVIĆ, M. Carbonation of cement paste: understanding, challenges, and opportunities. **Construction and Building Materials**, v. 117, p. 285–301, 2016.
- SCRIVENER, K.; SNELLINGS, R.; LOTHENBACH, B. **A practical guide to microstructural analysis of cementitious materials**. New York: CRC Press, 2016.
- SHIN, B.; KIM, S. CO₂ emission and construction cost reduction effect in cases of recycled aggregate utilized for nonstructural building materials in South Korea. **Journal of Cleaner Production**, v. 360, p. 131962, 2022.
- SINDICATO NACIONAL DA INDÚSTRIA DO CIMENTO. **Dados do setor**. São Paulo. 2022. Available: <http://snic.org.br/numeros-do-setor.php>. Access: 01 jan. 2023.
- STEIN, T. **NOAA index tracks how greenhouse gas pollution amplified global warming in 2022**. 2023. Available: <https://research.noaa.gov/2023/05/23/noaa-index-tracks-how-greenhouse-gas-pollution-amplified-global-warming-in-2022/>. Access: 26 mar. 2024.
- TAVARES, S. F.; BRAGANÇA, L. Índices de CO₂ para materiais de construção em edificações brasileiras. In: SUSTAINABLE URBAN COMMUNITIES TOWARDS A NEARLY ZERO IMPACT BUILT ENVIRONMENT, Minho, 2016. **Proceedings [...]** Minho, 2016.
- THOMAZ, W. de A.; MIYAJI, D. Y.; POSSAN, E. Comparative study of dynamic and static Young's modulus of concrete containing basaltic aggregates. **Case Studies in Construction Materials**, v. 15, p. e00645, 2021.
- TUUTTI, K. **Corrosion of steel in concrete**. Stockholm: Swedish cement and concrete research institute, 1982.
- VILLAIN, G.; THIERY, M.; PLATRET, G. Measurement methods of carbonation profiles in concrete: Thermogravimetry, chemical analysis and gammadensimetry. **Cement and Concrete Research**, v. 37, n. 8, p. 1182–1192, 2007.

WANG, J.; MU, M.; LIU, Y. Recycled cement. **Construction and Building Materials**, v. 190, p. 1124–1132, 2018.

WANG, L. *et al.* Eco-friendly treatment of recycled concrete fines as supplementary cementitious materials. **Construction and Building Materials**, v. 322, p. 126491, 2022.

WIJAYASUNDARA, M.; MENDIS, P.; NGO, T. Comparative assessment of the benefits associated with the absorption of CO₂ with the use of RCA in structural concrete. **Journal of Cleaner Production**, v. 158, p. 285–295, 2017.

XUAN, D.; ZHAN, B.; POON, C. S. Assessment of mechanical properties of concrete incorporating carbonated recycled concrete aggregates. **Cement and Concrete Composites**, v. 65, p. 67–74, 2016.

YANG, K. H.; SEO, E. A.; TAE, S. H. Carbonation and CO₂ uptake of concrete. **Environmental Impact Assessment Review**, v. 46, p. 43–52, 2014.

Acknowledgments

The authors would like to thank Itaipu, the Itaipu Concrete Technology Laboratory and Unioeste, for their support in the experimental project, and the Unioeste Foundation and PRPPG | Unila for its research support.

Beatrice Lorenz Fontolan

Conceptualization, Methodology, Writing, Data analysis.

Engenharia Civil | Universidade Tecnológica Federal do Paraná | Rua Dep. Heitor Alencar Furtado, 5000,- Cidade Industrial de Curitiba | Curitiba - PR - Brasil | CEP 81280-340 | Tel.: (41) 3279-6800 | E-mail: fontolanbeatrice@gmail.com

Taine Beal Silva

Data analysis.

Engenharia Civil | Universidade Tecnológica Federal do Paraná | Via do Conhecimento, KM 01, Fraron | Pato Branco - PR - Brasil | CEP 85503-390 | Tel.: (46) 3220-2511 | E-mail: tainebs@hotmail.com

Giovanna Patrícia Gava

Supervision.

Engenharia Civil | Universidade Estadual do Oeste do Paraná | Rua Universitária, 2069, Universitário | Cascavel - PR - Brasil | CEP 85819-110 | Tel.: (45) 3220-3000 | E-mail: gpgava@gmail.com

Eduardo Rigo

Supervision.

Engenharia Civil | Universidade Federal da Integração Latino-Americana | Av. Tarquínio Joslin dos Santos, 1000 | Foz do Iguaçu - PR - Brasil | CEP 85870-650 | Tel.: (45) 3522-9695 | E-mail: eduardorigo.e@gmail.com

Alex Neves Junior

Critical review.

Engenharia Civil | Universidade Federal de Mato Grosso | Avenida Fernando Correa de Costa, 2367, Boa Esperança | Cuiabá - MT - Brasil | CEP 78060-900 | Tel.: (65) 3615-8000 | E-mail: alex.junior@ufmt.br

Edna Possan

Supervision, Critical Review.

Engenharia Civil | Universidade Federal da Integração Latino-Americana | E-mail: epossan@gmail.com

Editor: **Marcelo Henrique Farias de Medeiros**

Ambiente Construído

Revista da Associação Nacional de Tecnologia do Ambiente Construído

Av. Osvaldo Aranha, 99 - 3º andar, Centro

Porto Alegre - RS - Brasil

CEP 90035-190

Telefone: +55 (51) 3308-4084

www.seer.ufrgs.br/ambienteconstruido

www.scielo.br/ac

E-mail: ambienteconstruido@ufrgs.br



This is an open-access article distributed under the terms of the Creative Commons Attribution License.